Density functional theory of freezing: Analysis of crystal density

ARTICLE *in* THE JOURNAL OF CHEMICAL PHYSICS · OCTOBER 1987

Impact Factor: 2.95 · DOI: 10.1063/1.453663

3 AUTHORS:

Brian B. Laird
University of Kansas
120 PUBLICATIONS **3,440** CITATIONS
SEE PROFILE

John Mccoy
New Mexico Institute of Mining and Techno…
114 PUBLICATIONS **2,021** CITATIONS
SEE PROFILE

A. D. J. Haymet
University of California, San Diego
201 PUBLICATIONS **6,347** CITATIONS
SEE PROFILE

Density functional theory of freezing: Analysis of crystal density

Brian B. Laird, John D. McCoy, and A. D. J. Haymet
Department of Chemistry, University of California, Berkeley, California 94720

(Received 1 June 1987; accepted 21 July 1987)

The density functional theory of freezing is used to study the liquid to crystal phase transition in the hard-sphere and Lennard-Jones systems. An important step in the calculation is the parametrization of the solid phase average single particle density $\rho(\mathbf{r})$. In this work two popular parametrizations are compared. The first method is a general Fourier decomposition of the periodic solid density in which the amplitude of each (non-symmetry-related) Fourier component is treated as an independent parameter. The second parametrization, which is more restrictive but easier to implement, approximates the solid density as a sum of Gaussian peaks centered at the sites of a periodic lattice. The two methods give essentially identical results for the phase diagrams for the two systems studied, but the crystal density predicted by the Fourier method exhibits significant anisotropies which are excluded from the Gaussian representation by construction.

I. INTRODUCTION

Density functional theory of classical statistical mechanics[1–4] has become an important tool in the study of first-order phase transitions from first principles. In various forms the theory has been used to describe and predict the freezing of simple liquids into periodic[5–15] and quasiperiodic[16,17] solids, the freezing of binary mixtures,[18,19] the structure[20–26] and dynamics[27,28] of solid–liquid interfaces, the liquid to glass transition,[29,30] liquid to solid nucleation,[31,32] and the elastic properties of solids near their melting point.[33]

The primary goal of the freezing theory is to predict the thermodynamic conditions at which phase coexistence between a solid and a liquid is possible. The thermodynamic properties of the solid are obtained by calculating the crystal phase correlation functions perturbatively from the correlation functions of the bulk liquid. This idea originates in the work of Kirkwood and Monroe,[34] who developed a canonical ensemble formalism using the pair correlation function $g(r)$. Ramakrishnan and Yussouff[5] (RY) constructed a freezing theory using the grand canonical ensemble, and Haymet and Oxtoby,[20] in the course of studying the structure of the crystal–liquid interface, recast the RY theory into the language of density functional theory and the pair direct correlation function $c(r)$.

Once the properties of the solid are calculated, the freezing point is determined from the condition that the liquid and the solid must be in thermal and mechanical equilibrium; that is, the temperature, chemical potential, and pressure of the liquid phase are equal to the corresponding solid phase quantities. The equality of the temperatures and of the chemical potentials are assumed *a priori* by the use of the grand canonical ensemble, in which the natural variables are temperature, chemical potential, and volume. The pressures are set equal by varying the liquid density until the grand thermodynamic potential, $\beta\Omega = -pV/kT$, of the solid phase equals that of the liquid phase.

It should be noted that in an exact treatment of the equilibrium statistical mechanics of freezing there would not be two states of a system at the same temperature and chemical potential which have different pressures. The density functional theory predicts a range of liquid densities for which there is a solid solution, because it assumes that the system is either all liquid or all solid; that is, it ignores fluctuations in which the two phases coexist within the same sample. This mean-field or "homogeneity" approximation and its relation to van der Waals theory is discussed in depth by Haymet and Oxtoby.[35]

In addition to the liquid correlation functions, some information about the solid phase density must be supplied as input. Since the present theory is not able to solve the problem of "spontaneous translational symmetry breaking," the space group symmetry of the solid must be assumed in advance of the calculation. The equilibrium crystal symmetry is determined by performing the calculation for a set of plausible structures and chosing the one with the lowest value for the free energy.

In addition to the symmetry, the actual shape of the single particle density about the lattice sites must be parametrized. Two parametrizations are used extensively in density functional freezing calculations. The easiest to implement is a quasiharmonic approximation whereby the density about each lattice site is assumed to be isotropic *and* Gaussian. In this *Gaussian method*, introduced by Jacobs,[9] there are only two parameters which describe the solid density: the lattice spacing and the Gaussian width. The other method used in the original calculations by Ramakrishnan and Yussouff,[5] and Haymet and Oxtoby,[20] is a general Fourier decomposition where each nonsymmetry-related Fourier component of the solid density is treated as an independent variable. This *Fourier method* is less approximate and more difficult to implement than the Gaussian method, but of course it has the added ability to explore possible anharmonicities and anisotropies of the density. The principal purpose of this paper is to compare and contrast the difference in the freezing results obtained using these two methods.

In addition, we assume here that there is exactly one particle per lattice site. This is the "perfect crystal" assumption, discussed by Haymet and Oxtoby.[35] The Gaussian method calculations of Jones and Mohanty[10] on the hard-sphere system permit the lattice sites to be partially occupied, and any deviation from the perfect crystal condition is

 0021-9606/87/215449-08$02.10

interpreted as indicating the presence of defects (vacancies or interstitials). Since the input to the theory contains no information about defect–defect or defect–particle correlations, it seems unrealistic to expect it to yield any information about equilibrium defects in the solid.

The density functional theory of freezing is summarized in Sec. II, but it is by no means comprehensive and the reader is encouraged to consult one of the reviews[1–4] for a more complete treatment of the subject. Sections III and IV discuss the details of the Gaussian and Fourier methods, respectively. Freezing results for hard spheres are presented in Sec. V and those for the Lennard-Jones system in Sec. VI.

II. THE DENSITY FUNCTIONAL THEORY OF FREEZING

Consider a system of classical particles of mass m with temperature T, volume V, and chemical potential μ. The particles interact via a potential energy $U(\mathbf{r}_1,...,\mathbf{r}_n)$ and feel an external single particle potential $\phi(\mathbf{r})$. Defining a dimensionless single particle effective potential by

$$u(\mathbf{r}) = \beta\mu - \beta\phi(\mathbf{r}), \tag{2.1}$$

we write the grand canonical partition function

$$Z_G = \exp(-\beta\Omega) = \sum_{N=0}^{\infty} \frac{1}{N!\Lambda^{3N}} \int d\mathbf{r}_1 \cdots d\mathbf{r}_N \times \exp\left\{-\beta U + \sum_{i=1}^{N} u(\mathbf{r}_i)\right\}, \tag{2.2}$$

where $\beta\Omega = -pV/k_BT$, $\beta = 1/k_BT$, and $\Lambda = (\beta h^2/2\pi m)^{1/2}$.

The free energy $\beta\Omega$ is a natural functional of $u(\mathbf{r})$ with

$$\frac{\delta\beta\Omega}{\delta u(\mathbf{r})} = -\rho(\mathbf{r}), \tag{2.3}$$

where

$$\rho(\mathbf{r}) = \left\langle \sum_{i=1}^{N} \delta(\mathbf{r} - \mathbf{r}_i) \right\rangle \tag{2.4}$$

and the $\langle \cdots \rangle$ denote a grand canonical equilibrium average. One of the principal results of density functional theory is that there exists a functional $\beta\tilde{\Omega}([u(\mathbf{r})],[\rho(\mathbf{r})])$ which, when minimized with respect to $\rho(\mathbf{r})$ at fixed $u(\mathbf{r})$, gives $\beta\Omega[u]$[1,2]:

$$\beta\Omega[u] = \min_{\rho(\mathbf{r})}\{\beta\tilde{\Omega}([u],[\rho])\}. \tag{2.5}$$

The function $\rho(\mathbf{r})$ which minimizes $\beta\tilde{\Omega}$ is identified as the true equilibrium single particle density defined by Eq. (2.4).

The functional $\beta\tilde{\Omega}([u],[\rho])$, relative to some reference state characterized by potential $u_r(\mathbf{r})$ and density $\rho_r(\mathbf{r})$, can be written as the sum of an ideal gas term, $\Delta\beta\tilde{\Omega}_{\text{ideal}}$, and a term which reflects the interparticle interactions, $\Delta\beta\tilde{\Omega}_{\text{int}}$:

$$\Delta\beta\tilde{\Omega} = \beta\tilde{\Omega}([u],[\rho]) - \beta\tilde{\Omega}([u_r],[\rho_r]) = \Delta\beta\tilde{\Omega}_{\text{ideal}} + \Delta\beta\tilde{\Omega}_{\text{int}} \tag{2.6}$$

with

$$\Delta\beta\tilde{\Omega}_{\text{ideal}} = \int_V d\mathbf{r}\{\rho(\mathbf{r})\ln[\rho(\mathbf{r})/\rho_r(\mathbf{r})] + \rho(\mathbf{r})[u(\mathbf{r}) - u_r(\mathbf{r})] - [\rho(\mathbf{r}) - \rho_r(\mathbf{r})]\} \tag{2.7}$$

and

$$\Delta\beta\tilde{\Omega}_{\text{int}} = -\sum_{n=2}^{\infty} \frac{1}{n!} \int_V d\mathbf{r}_1 \cdots d\mathbf{r}_n\, C_r^{(n)}(\mathbf{r}_1,...,\mathbf{r}_n) \times [\rho(\mathbf{r}_1) - \rho_r(\mathbf{r}_1)] \cdots [\rho(\mathbf{r}_n) - \rho_r(\mathbf{r}_n)]. \tag{2.8}$$

The functions $C^{(n)}(\mathbf{r}_1,...,\mathbf{r}_n)$ are the n-particle direct correlation functions of the reference state and are defined by

$$C_r^{(n)}(\mathbf{r}_1,...,\mathbf{r}_n) = \delta^{(n)}\left\{\int_V d\mathbf{r}\,\rho_r(\mathbf{r})[\ln\rho_r(\mathbf{r}) - 1] - F[\rho_r]\right\}/\delta\rho_r(\mathbf{r}_1)...\delta\rho_r(\mathbf{r}_n), \tag{2.9}$$

where the Legendre transform of $\beta\Omega[u]$,

$$F[\rho] = \beta\Omega[u] + \int_V d\mathbf{r}\,\rho(\mathbf{r})u(\mathbf{r}), \tag{2.10}$$

is β times the Helmholtz free energy A minus the average total external potential energy

$$F[\rho] = \beta\left[A - \int d\mathbf{r}\,\rho(\mathbf{r})\phi(\mathbf{r})\right]. \tag{2.11}$$

In this calculation, the reference system is taken to be the equilibrium liquid phase at a uniform density $\rho_r(\mathbf{r}) = \rho_L$ which has the same chemical potential as the solid phase represented by $\rho(\mathbf{r})$. The external potential of both systems is set to zero. These two conditions imply

$$u(\mathbf{r}) - u_r(\mathbf{r}) = 0. \tag{2.12}$$

It should be noted that it is not necessary that the coexisting liquid be used as the reference system. Igloi and Hafner[12] use a uniform reference liquid which has a different chemical potential than the coexisting liquid and solid phases. The reference liquid is chosen so that the minimized $\Delta\beta\tilde{\Omega}$ is a minimum with respect to the reference liquid density. This criterion yields a reference liquid density which is slightly lower than the coexisting liquid density. Baus and Colot[11] chose a reference density with the requirement that the first peak in the structure factor $S(k)$ coincides with the position of the first reciprocal lattice vector of the solid phase.

Assuming that the solid correlation functions can be well described by those of the liquid, the expansion in $\Delta\beta\tilde{\Omega}_{\text{int}}$ is retained only to second order in the density difference $\rho(r) - \rho_L$. Identifying $C^{(2)}(\mathbf{r}_1,\mathbf{r}_2)$ as the Ornstein–Zernike two-particle direct correlation function, $c(|\mathbf{r}_1 - \mathbf{r}_2|)$, we obtain the following expression for $\Delta\beta\tilde{\Omega}$:

$$\Delta\beta\tilde{\omega} = \frac{\Delta\beta\tilde{\Omega}}{\rho_L V} = \frac{1}{\rho_L V}\int d\mathbf{r}_1\{\rho(\mathbf{r}_1)\ln[\rho(\mathbf{r}_1)/\rho_L] - [\rho(\mathbf{r}_1) - \rho_L]\} - \frac{1}{2\rho_L V}\int d\mathbf{r}_1\,d\mathbf{r}_2 \times c(|\mathbf{r}_1 - \mathbf{r}_2|)[\rho(\mathbf{r}_1) - \rho_L][\rho(\mathbf{r}_2) - \rho_L]. \tag{2.13}$$

After the functional (2.13) has been minimized using

one of the procedures outlined in Secs. III or IV, the liquid density is varied until the value of $\Delta\beta\omega = \Delta\beta\tilde{\omega}_{\min}$ is zero; this identifies the freezing point unambiguously.

III. THE GAUSSIAN APPROXIMATION

A simple parametrization for the solid density is based on the fact that the potential energy of a particle about its crystal lattice site is approximately harmonic. The density can be then represented by a sum of Gaussians at each lattice site:

$$\rho(\mathbf{r}) = (\pi\epsilon^2)^{-3/2} \sum_{\{\mathbf{R}_n\}} \exp[-(|\mathbf{R}_n - \mathbf{r}|)^2/\epsilon^2], \quad (3.1)$$

where the vectors $\{\mathbf{R}_n\}$ are the real-space crystal lattice vectors and ϵ is a measure of the width of the Gaussian peaks.

Following Tarazona,[14] Jacobs,[9] and Jones and Mohanty,[10] $\Delta\beta\tilde{\omega}$ takes on a simple form if the Gaussians are assumed to be nonoverlapping. This assumption, necessary for the evaluation of the $\rho \ln \rho$ integral in $\Delta\beta\tilde{\omega}_{\text{ideal}}$, is accurate to a very high degree for the range of solid densities and Gaussian widths which are considered in all calculations contained in this paper. The integral over $c(|\mathbf{r}_1 - \mathbf{r}_2|)$ is more convienently evaluated by decomposing the Gaussian density in a Fourier series since the integral becomes a sum over reciprocal lattice vectors and $c(r)$ is replaced by its Fourier transform, $c(k)$, which is easily obtained from experiments and computer simulations via the structure factor, $S(k)$:

$$c(|\mathbf{k}|) = \rho \int d\mathbf{r}\, e^{i\mathbf{k}\cdot\mathbf{r}} c(r) = 1 - \frac{1}{S(k)}. \quad (3.2)$$

Substituting the parametrization (3.1) into Eq. (2.13) then gives

$$\Delta\beta\tilde{\omega} = 1 - (1+\eta)[5/2 + \ln\rho_L + 3/2 \ln(\pi\epsilon^2)] - \frac{1}{2}\eta^2 c(0) - \frac{1}{2}\sum_{\{\mathbf{k}_n\}} \mu^2(|\mathbf{k}_n|) c(|\mathbf{k}_n|) - \frac{1}{6}\eta^3 c^{(3)}(0,0), \quad (3.3)$$

where η is the fractional density change on freezing,

$$\eta = (\rho_S - \rho_L)/\rho_L, \quad (3.4)$$

and $\rho_L \mu(\mathbf{k}_n)$ is the Fourier component of the density corresponding to the (nonzero) reciprocal lattice vector $\mathbf{k}_n$,

$$\rho(r) = \rho_L \left[1 + \eta + \sum_{\{\mathbf{k}_n\}} \mu(\mathbf{k}_n) e^{i\mathbf{k}_n\cdot\mathbf{r}}\right]. \quad (3.5)$$

For the Gaussian density, Eq. (3.1),

$$\mu_G(\mathbf{k}_n) = (1+\eta)\exp(-|\mathbf{k}_n|^2\epsilon^2/4). \quad (3.6)$$

The last term in Eq. (3.3) does not come from Eq. (2.13), but is the zero wave vector contribution of the term in Eq. (2.8) where n equals 3. This term involves the three-particle direct correlation function of the liquid, which is in general unknown. When evaluating this integral using the Fourier decomposion, the only Fourier components of $C^{(3)}(\mathbf{r}_1,\mathbf{r}_2,\mathbf{r}_3)$ which contribute are those whose three wave vectors form a closed triangle; so, we can define the Fourier transform of $C^{(3)}$ as

$$c^{(3)}(\mathbf{k}_1,\mathbf{k}_2) = \rho_L^2 V^{-1} \int_V d\mathbf{r}_1\, d\mathbf{r}_2\, d\mathbf{r}_3\, e^{i\mathbf{k}_1\cdot\mathbf{r}_1} e^{i\mathbf{k}_2\cdot\mathbf{r}_2} \times e^{-i(\mathbf{k}_1+\mathbf{k}_2)\cdot\mathbf{r}_3} C^{(3)}(\mathbf{r}_1, \mathbf{r}_2, \mathbf{r}_3). \quad (3.7)$$

Accurate values for $c^{(3)}(\mathbf{k}_1, \mathbf{k}_2)$ where both $\mathbf{k}_1$ and $\mathbf{k}_2$ are nonzero are difficult to obtain, but if one or both of the wave vectors are zero, then the triplet term can be calculated as a density derivative of the two-particle function

$$c^{(3)}(k,0) = \rho \frac{\partial c(k)}{\partial \rho} - c(k). \quad (3.8)$$

Only the $c^{(3)}(0,0)$ term is included in Eq. (3.3) since Haymet[6] has shown that, at least in the case of hard spheres, as the magnitude of $\mathbf{k}$ increases the terms with one nonzero $\mathbf{k}$ oscillate in sign in such a way that their contributions to the freezing results tend to cancel each other.

At a given liquid density, $\Delta\beta\tilde{\omega}$ for the Gaussian solid, as given by Eqs. (3.3) and (3.6), is a function of only two parameters, ϵ and η. Minimization with respect to these two quantities is straightforward.

IV. THE FOURIER EXPANSION

This minimization procedure utilizes the Fourier expansion for the solid density, Eq. (3.5), but unlike the Gaussian method which has only two parameters, each non-symmetry-related Fourier component is allowed to vary independently. Since this decomposition spans the space of all possible density functions consistent with the crystal symmetry, the Fourier method is much more general than the Gaussian method and can address possible anharmonicities and anisotropies of the solid density. This greater generality together with the variational theorem for $\Delta\beta\tilde{\omega}$ leads to the conclusion that for a given liquid density the minimum value of $\Delta\beta\tilde{\omega}$ calculated with the Fourier method should be less than or equal to the corresponding Gaussian method value:

$$\Delta\beta\tilde{\omega}_{\min}^{\text{Fourier}}(\rho_L) \leqslant \Delta\beta\tilde{\omega}_{\min}^{\text{Gaussian}}(\rho_L). \quad (4.1)$$

As illustrated in Fig. 1, Eq. (4.1) together with the negativity of the slope of $\Delta\beta\tilde{\omega}_{\min}$ vs ρ_L (the solid becomes more

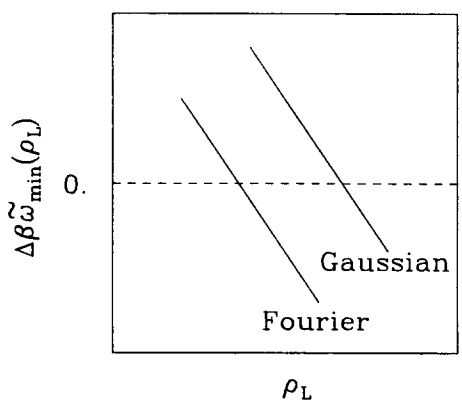

FIG. 1. A schematic diagram of the relative positions of the $\Delta\beta\tilde{\omega}_{\min}(\rho_L)$ curves for the Fourier and Gaussian methods. The density at which each curve crosses zero (the dotted line) is the predicted liquid freezing density for that method.

stable at higher densities) implies that the Fourier method will give a liquid freezing density which is less than or equal to the Gaussian freezing density.

All calculations to date which use the full Fourier decomposition[6–8,12] determine the Fourier components of the minimum density by solving the extremum equation

$$\frac{\delta\Delta\beta\tilde{\omega}}{\delta\rho(\mathbf{r})}=0, \tag{4.2}$$

which together with Eq. (2.13) yields

$$\ln[\rho(\mathbf{r}_1)/\rho_L]=\int_V d\mathbf{r}_2\, c(|\mathbf{r}_1-\mathbf{r}_2|)[\rho(\mathbf{r}_2)-\rho_L]. \tag{4.3}$$

Equation (4.3) can be solved by exponentiating both sides and projecting out the individual Fourier components. The functional $\Delta\beta\tilde{\omega}$ can be evaluated at its extremum by substituting Eq. (4.3) into Eq. (2.13), giving

$$\begin{aligned}\Delta\beta\tilde{\omega}_{\min}=&-\frac{1}{\rho_L V}\int_V d\mathbf{r}_1[\rho(\mathbf{r}_1)-\rho_L]\\&+\frac{1}{2\rho_L V}\int_V d\mathbf{r}_1\, d\mathbf{r}_2\, c(|\mathbf{r}_1-\mathbf{r}_2|)\\&\times[\rho(\mathbf{r}_2)-\rho_L][\rho(\mathbf{r}_1)+\rho_L].\end{aligned} \tag{4.4}$$

Equation (4.3) is a necessary condition for the true minimum but is not a sufficient one, since a saddle point or maximum satisfies the same equation. In fact, it has been discovered that the true minimum solution lies off of the perfect crystal constraint. Since all previous uses of this method assume a perfect crystal (or at least make some other connection between ρ_s and the lattice constant a_{lat}) when implementing Eq. (4.3), the density obtained, while satisfying the extremum condition, cannot be the true minimum. The density obtained by this procedure is not even the minimum on the perfect crystal constraint surface. Evidence of this can be seen in the observation that the Gaussian method, which is a true constrained minimization, gives a lower freezing density than the Fourier method, a fact which contradicts condition (4.1).

The correct way to implement the Fourier method within the perfect crystal approximation is to do a constrained minimization with a Lagrange multiplier. This involves defining a new functional, $\Delta\tilde{\omega}'[\rho]$, which is $\Delta\tilde{\omega}[\rho]$ minus a Lagrange multiplier λ times a term which is zero when the constraint is satisfied:

$$\begin{aligned}\Delta\beta\tilde{\omega}'[\rho]=&\frac{1}{\rho_L\Delta}\int_\Delta d\mathbf{r}_1\{\rho(\mathbf{r}_1)\ln[\rho(\mathbf{r}_1)/\rho_L]\\&-[\rho(\mathbf{r}_1)-\rho_L]\}-\frac{1}{2\rho_L\Delta}\\&\times\int_V\int_\Delta d\mathbf{r}_1\, d\mathbf{r}_2\, c(|\mathbf{r}_1-\mathbf{r}_2|)\\&\times[\rho(\mathbf{r}_1)-\rho_L][\rho(\mathbf{r}_2)-\rho_L]\\&-\frac{\lambda}{\rho_L\Delta}\left[\int_\Delta d\mathbf{r}_1\rho(\mathbf{r}_1)-N_\Delta\right],\end{aligned} \tag{4.5}$$

where Δ is the volume of the unit cell and N_Δ is the number of particle sites per unit cell. The perfect crystal condition is expressed by the constraint equation

$$\int_\Delta d\mathbf{r}_1\rho(\mathbf{r}_1)-N_\Delta=0; \tag{4.6}$$

that is, there are no partially occupied sites. The minimization of $\Delta\beta\tilde{\omega}$ subject to the constraint is accomplished by solving the equation

$$\frac{\delta\Delta\beta\tilde{\omega}'}{\delta\rho(\mathbf{r}_1)}=0 \tag{4.7}$$

simultaneously with Eq. (4.6).

Minimizing Eq. (4.5) we obtain

$$\ln[\rho(\mathbf{r}_1)/\rho_L]=\lambda+\int_V d\mathbf{r}_2\, c(|\mathbf{r}_1-\mathbf{r}_2|)[\rho(\mathbf{r}_2)-\rho_L] \tag{4.8}$$

with

$$\begin{aligned}\Delta\beta\tilde{\omega}'_{\min}=&-\frac{1}{\rho_L\Delta}\int_\Delta d\mathbf{r}_1[\rho(\mathbf{r}_1)-\rho_L]\\&+\frac{1}{2\rho_L\Delta}\int_V\int_\Delta d\mathbf{r}_1\, d\mathbf{r}_2\, c(|\mathbf{r}_1-\mathbf{r}_2|)\\&\times[\rho(\mathbf{r}_2)-\rho_L][\rho(\mathbf{r}_1)+\rho_L]\\&+\frac{\lambda}{\rho_L\Delta}\int_\Delta d\mathbf{r}_1\rho(\mathbf{r}_1).\end{aligned} \tag{4.9}$$

Exponentiating both sides of Eq. (4.8) and converting the real-space integration into a Fourier space sum over reciprocal lattice vectors yields the following equation for the solid density:

$$\begin{aligned}\rho(\mathbf{r})=\rho_L\exp\Big\{&\lambda+c(0)\eta+\tfrac{1}{2}c^{(3)}(0,0)\eta^2\\&+\sum_{\{\mathbf{k}_n\}}c(|\mathbf{k}_n|)\mu(\mathbf{k}_n)e^{i\mathbf{k}_n\cdot\mathbf{r}}\Big\},\end{aligned} \tag{4.10}$$

where the $c^3(0,0)$ term appears for the reasons discussed in the previous section. To solve this equation for λ and the Fourier parameters η and $\{\mu_n\}$ the sum is truncated after a finite number of reciprocal lattice vector sets, $n_{\max}$, which is large enough to give convergence in the freezing results. The Fourier components of both sides are then projected out to yield a set of $n_{\max}$, nonlinear equations

$$\begin{aligned}&\mu(\mathbf{k}_j)+\delta_{\mathbf{k}_j,0}\\&=\int_\Delta\frac{d\mathbf{r}}{\Delta}e^{-i\mathbf{k}_j\cdot\mathbf{r}}\exp\Big\{\lambda+c(0)\eta\\&\quad+\frac{1}{2}c^{(3)}(0,0)\eta^2+\sum_{\{\mathbf{k}_n\}}c(|\mathbf{k}_n)\mu(\mathbf{k}_n)e^{i\mathbf{k}_n\cdot\mathbf{r}}\Big\},\end{aligned} \tag{4.11}$$

where $\mu(\mathbf{k}=\mathbf{0})=\eta$. Equation (4.11) together with the constraint equation

$$\rho_L(1+\eta)=\frac{N_\Delta}{\Delta} \tag{4.12}$$

can now be solved to determine the solid density. The functional $\Delta\beta\tilde{\omega}'_{\min}$ is evaluated using Eq. (4.9) which after Fourier decomposition becomes

$$\Delta\beta\tilde{\omega}'_{\min} = [c(0)-1]\eta + \tfrac{1}{2}[c(0)+c^{(3)}(0,0)]\eta^2 + \tfrac{1}{3}c^{(3)}(0,0)\eta^3 + \frac{1}{2}\sum_{\{\mathbf{k}_n\}} c(|\mathbf{k}_n|)\mu^2(\mathbf{k}_n) + \lambda(1+n). \quad (4.13)$$

In this form, $\Delta\beta\tilde{\omega}'_{\min}$ is minimized with respect to the unit cell volume Δ to give the perfect crystal contrained minimum of $\Delta\beta\tilde{\omega}$.

Note that the truncation in Eq. (4.10) is justified by the fact that the product $c(\mathbf{k}_n)\mu(\mathbf{k}_n)$ approaches zero for large amplitude wave vectors. The convergence of the sum in Eq. (4.10) is much faster than in Eq. (3.5) where the order parameters $\mu(\mathbf{k}_n)$ appear alone. Also, the density calculated from a falsely truncated Eq. (3.5) can have large negative regions unlike Eq. (4.10) which is inherently positive. As shown previously,[36] only Eq. (4.10) yields the correct crystal density.

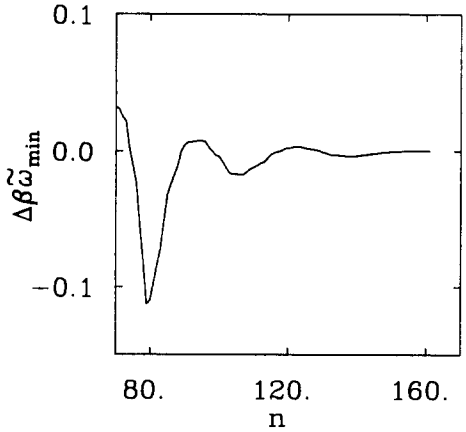

FIG. 2. The convergence of $\Delta\beta\tilde{\omega}_{\min}(\rho_L)$ vs the number $n_{\max}$ of order parameters included in the hard-sphere calculation. The liquid density and unit cell volume used are such as to give a freezing solution at $n_{\max} = 161$.

V. HARD-SPHERE RESULTS

The hard-sphere system is the standard first testing ground for density functional theories of freezing. The system has several advantages, and a crucial disadvantage. First, the freezing line of the phase diagram depends only upon the density, and not upon both the density and the temperature as in most other systems. This simplifies the study since the entire phase diagram is determined from only one freezing calculation. Another advantage is that approximate but accurate liquid structure information is available in analytic form. Unfortunately, the unphysical discontinuity in the direct correlation function introduces a pathology into the formalism.

Particles in the hard-sphere model interact via the spherically symmetric pairwise additive potential

$$u(r) = \begin{cases} \infty & r < \sigma \\ 0 & r \geqslant \sigma \end{cases}. \quad (5.1)$$

For the remainder of this section the following reduced units will be used: reduced radial distance $r^* = r/\sigma$, and reduced density $\rho^* = \rho\sigma^3$.

The hard-sphere two-particle direct correlation function $c(r)$ used in this and earlier calculations is the exact analytic solution to the Percus–Yevick[37] equation. This $c(r)$, derived by Wertheim and Thiele,[38] is given by

$$c(r^*) = \begin{cases} (1+\tfrac{1}{2}\xi r^{*3})\lambda_1 + 6\xi r^*\lambda_2 & r^* < 1 \\ 0 & r^* \geqslant 1 \end{cases}, \quad (5.2)$$

where the packing fraction $\xi = \pi\rho^*/6$, $\lambda_1 = (1+2\xi)^2/(1-\xi)^4$, and $\lambda_2 = -(1+\xi/2)^2/(1-\xi)^4$.

The system is assumed to freeze into a face-centered-cubic (fcc) crystal. This is the crystal structure seen in the computer simulations.[39] Whether the equilibrium hard sphere crystal is in fact fcc or the closely related hexagonal-close-packed (hcp) structure is at present unresolved. Preliminary calculations by the authors show that, at least for the Gaussian method, the difference in the freezing parameters between hcp and fcc is negligible for the hard-sphere system.

The Gaussian calculation uses 200 sets of reciprocal lattice vectors, whereas 161 sets are used for the Fourier calculation. Figure 2 illustrates the convergence of $\Delta\beta\tilde{\omega}'_{\min}$ using the Fourier method at the calculated freezing density. The calculated freezing parameters for both methods are displayed in Table I together with the computer simulation results. The quantity L is the Sutherland[40]–Lindemann[41] ratio, which is defined to be the average root-mean-square deviation of a crystal particle from its lattice site divided by the nearest neighbor distance d_{nn},

$$L^2 = d_{nn}^{-2}\int_{\text{peak}} d\mathbf{r}\, r^2\rho(\mathbf{r}), \quad (5.3)$$

where the integral is over one crystal density peak. For the Gaussian approximation, it can be shown that

$$L = \sqrt{3/2}\epsilon/d_{nn}. \quad (5.4)$$

The empirical "rule" (which actually describes a crystal "instability") states that a crystal melts when L exceeds 10%, and this turns out to be true for many simple materials. Using this standard, the Fourier value of L is closer to 10%

TABLE I. Freezing parameters for hard spheres.

Method	Liquid density ρ_L	Crystal density ρ_S	Density change η	Gaussian width ϵ	Lindemann ratio L
Fourier	0.9836	1.1241	0.1429	···	0.065
Gaussian	0.9850	1.1258	0.1430	0.0520	0.059
Simulation (Ref. 39)	0.94–0.96	1.06–1.08	0.1	···	0.14

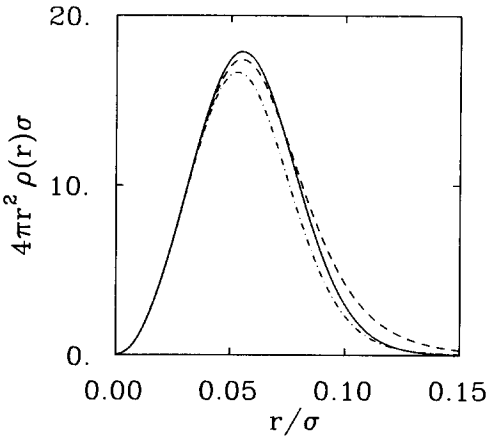

FIG. 3. The quantity $4\pi r^2\rho(\mathbf{r})$ at the hard-sphere Fourier freezing point in three different crystal directions: [100] (solid line), [110] (dashed line), and [111] (dotted line).

than the Gaussian value, but it is still quite low.

The results presented in Table I show that the Fourier and Gaussian methods give nearly identical results for ρ_L, ρ_S, and η. The difference in L indicates that the shape of the solid density peaks are measurably different. The Gaussian density is constrained to be isotropic, whereas the Fourier density is not so constrained. Figure 3 shows the Fourier density multiplied by the Jacobian factor $4\pi r^2$ in three different crystal directions: [100], [110], and [111]. Figure 4 shows the difference between these densities and the (isotropically constrained) Gaussian density.

VI. LENNARD-JONES RESULTS

Lennard-Jones particles[42] interact via the spherically symmetric, pairwise additive potential

$$u(r) = 4\epsilon\left[\left(\frac{\sigma}{r}\right)^{12} - \left(\frac{\sigma}{r}\right)^{6}\right], \tag{6.1}$$

where ϵ is the depth of the attractive well and σ is a measure of the particle size. This potential mimics the characteristics of the interaction potentials of rare gas elements and even more complicated molecules, namely an r^{-6} attraction at large distances and a steep repulsive wall at small distances. For the remainder of this section the following reduced units will be used: reduced distance $r^* = r/\sigma$, reduced density $\rho^* = \rho\sigma^3$, and reduced temperature $T^* = k_B T/\epsilon$. The liquid direct correlation function $c(k)$ is obtained by Fourier transformation of an analytic fit to the Lennard-Jones pair correlation function $g(r)$ obtained by Goldman[43] from an analysis of computer simulation data. Because this pair correlation function is only accurate for $r \lesssim 10\sigma$, the transform $c(k)$ obtained from it is badly behaved at small k. In light of this fact, $c(0)$ and $c^3(0,0)$ were obtained directly from a 33-parameter equation of state fit by Nicholas *et al.*,[44] using the same computer simulation data base used in the $g(r)$ fit.

The only exception to the above input is near the triple point. The qualities $c(0)$ and $c^3(0,0)$ are calculated using the mean spherical approximation[45] (MSA) for $c(k)$. This was done because the equation of state fit gives inaccurate values of these quantities near the triple point leading to a disappearance of the freezing solutions below $T^* = 0.8$.

As for hard spheres, an fcc structure is assumed for the Lennard-Jones crystal. A total of 140 reciprocal lattice vector sets are used in both the Fourier and Gaussian calculations. The Lennard-Jones calculations exhibit faster convergence than the hard spheres calculations because the $c(k)$ for hard spheres is much more long ranged than its Lennard-Jones counterpart (see Fig. 5), due to the Fourier transform of the unphysical discontinuity in the hard sphere $c(r)$. The freezing parameters for both the Fourier and Gaussian methods are displayed for a variety of temperatures in Table II. As for hard spheres, the freezing parameters calculated by the Gaussian method are very nearly identical to the Fourier method results. Figure 6 is the phase diagram of the Lennard-Jones system, and it includes the present calculation, coexistence data from both computer simulations of Lennard-Jones particles[46] and experiments on argon[47,48] ($\sigma = 3.405$ Å and $\epsilon/k_B = 119$ K) as well as the gas–liquid coexistence line calculated from the equation of state using the Maxwell construction. The theory compares quite well

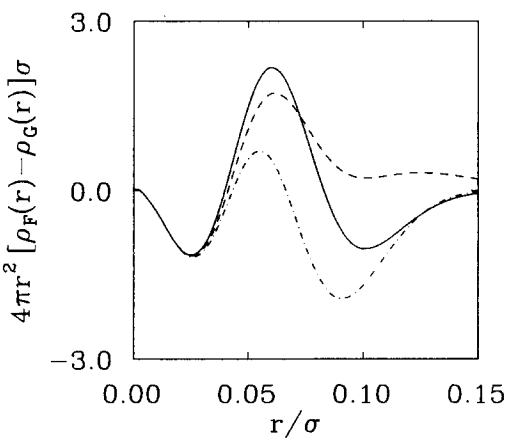

FIG. 4. The quantity $4\pi r^2[\rho_F(\mathbf{r}) - \rho_G(\mathbf{r})]$ at the hard-sphere freezing point in three different crystal directions: [100] (solid line), [110] (dashed line), and [111] (dotted line). $\rho_F(\mathbf{r})$ = Fourier method density. $\rho_G(\mathbf{r})$ = Gaussian method density.

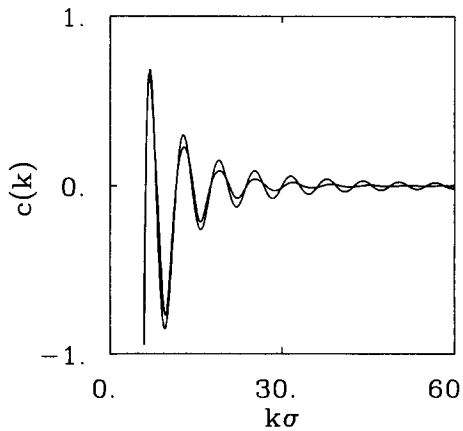

FIG. 5. The structure function $c(k)$ for the Lennard-Jones ($T^* = 1.3$) and hard-sphere (the more slowly decaying curve) liquids at their respective freezing densities.

TABLE II. Freezing parameters for Lennard-Jones system.

Temperature T	Method	Liquid density ρ_L	Crystal density ρ_S	Density change η	Gaussian width ϵ	Lindemann ratio L
0.72	Fourier	0.78	0.954	0.223	···	0.083
1.00	Fourier	0.877	1.017	0.159	···	0.086
	Gaussian	0.880	1.020	0.159	0.0677	0.074
1.15	Fourier	0.916	1.047	0.143	···	0.087
	Gaussian	0.918	1.050	0.144	0.0672	0.074
1.30	Fourier	0.947	1.074	0.134	···	0.087
	Gaussian	0.949	1.077	0.135	0.0670	0.075
1.60	Fourier	1.000	1.123	0.123	···	0.088
	Gaussian	1.002	1.126	0.124	0.0667	0.076
1.80	Fourier	1.030	1.153	0.119	···	0.089
	Gaussian	1.033	1.157	0.120	0.0662	0.076
2.00	Fourier	1.058	1.181	0.112	···	0.090
	Gaussian	1.060	1.185	0.118	0.0660	0.076
2.50	Fourier	1.117	1.243	0.112	···	0.090
	Gaussian	1.120	1.248	0.114	0.0655	0.077
2.74	Fourier	1.142	1.270	0.112	···	0.090
	Gaussian	1.144	1.273	0.113	0.0652	0.077
3.00	Fourier	1.168	1.298	0.112	···	0.090
	Gaussian	1.170	1.302	0.113	0.0647	0.077

with experiment, with the possible exception of predicting too high a value for the fractional density change η.

The Lennard-Jones system yields a much more isotropic Fourier solution for the crystal density than hard spheres (Fig. 7) but still displays a significant deviation from the Gaussian density (see Fig. 8). The values of the Lindemann ratios have the same Fourier to Gaussian relationship as hard spheres but are closer to the empirical value of 10%.

VII. CONCLUSIONS

There are a number of important technical conclusions from our study. First, we have demonstrated the correct implementation of the Fourier expansion of the crystal density, and the consistency of the subsequent minimization of the grand potential $\Delta\beta\Omega$. Secondly, we show that while the Fourier expansion and Gaussian approximation yield very similar phase diagrams for hard spheres and the Lennard-Jones system, there are measurable differences in the crystal densities predicted by the theory. This is shown to occur even in closed-packed crystals, where the Gaussian approximation, which forces crystal denisty isotropy, is presumably most correct. Even larger differences between the two methods are expected in more "open" crystal structures, such as body-centered-cubic (bcc) and the diamond lattice.

In the present calculations, properties which are directly related to the shape of the crystal density, such as the Lindemann ratio, display the greatest difference between the Fourier expansion and the Gaussian approximation. It would be worthwhile to examine by computer simulation the predicted anisotropy in the hard-sphere fcc crystal. Work is underway to study the difference between fcc and hcp close-

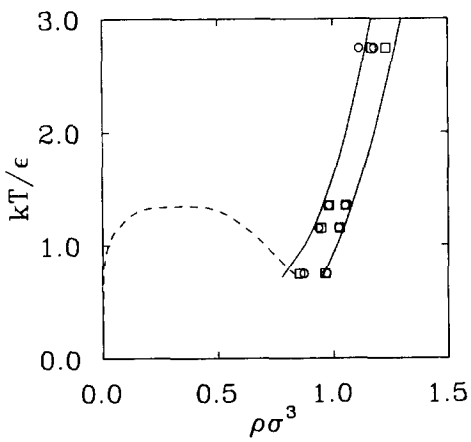

FIG. 6. The Lennard-Jones phase diagram displaying: the Fourier and Gaussian method density functional results (solid line); Monte Carlo simulation results (Ref. 46) (circles); experimental data for argon (Ref. 47) (squares); and the liquid–vapor coexistence line calculated from the Nicholas *et al.* (Ref. 44) equation of state by Maxwell construction (dashed line).

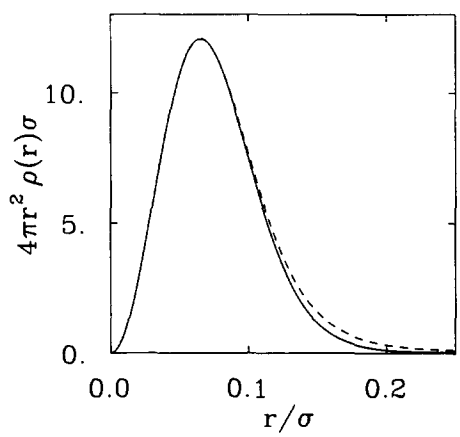

FIG. 7. The quantity $4\pi r^2\rho(r)$ at the Lennard-Jones, Fourier freezing point ($T^* = 1.3$) in three crystal directions: [110] (dashed line), [100] and [111] (solid line).

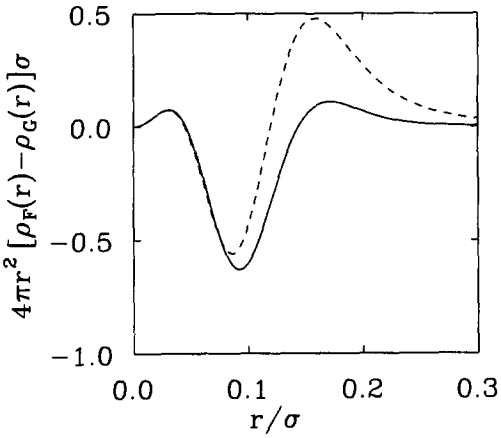

FIG. 8. The quantity $4\pi r^2[\rho_F(\mathbf{r}) - \rho_G(\mathbf{r})]$ at the Lennard-Jones freezing point ($T^* = 1.3$) in three different crystal directions: [110] (dashed line), [100] and [111] (solid line). $\rho_F(\mathbf{r})$ = Fourier method density. $\rho_G(\mathbf{r})$ = Gaussian method density.

packed crystals, and a variety of other substances and crystal types.

ACKNOWLEDGEMENTS

This work was supported in part by the NSF and the Ford Motor Company via the Presidental Young Investigator program. We thank Shep Smithline for many helpful discussions.

[1]J. L. Lebowitz and J. K. Percus, J. Math. Phys. **4**, 116 (1963).
[2]F. H. Stillinger and F. P. Buff, J. Chem. Phys. **37**, 1 (1962).
[3]D. Mermin, Phys. Rev. **137**, A 1441 (1965).
[4]R. Evans, Adv. Phys. **28**, 143 (1979).
[5]T. V. Ramakrishnan and M. Yussouff, Phys. Rev. B **19**, 2775 (1979).
[6]A. D. J. Haymet, J. Chem. Phys. **78**, 4641 (1983).
[7]S. J. Smithline and A. D. J. Haymet, J. Chem. Phys. **83**, 4103 (1985).
[8]C. Marshall, B. B. Laird, and A. D. J. Haymet, Chem. Phys. Lett. **122**, 320 (1985).
[9]R. L. Jacobs, J. Phys. C **16**, 273 (1983).
[10]G. Jones and U. Mohanty, Mol. Phys. **54**, 1241 (1985).
[11]M. Baus and J. L. Colot, Mol. Phys. **55**, 653 (1985).
[12]F. Igloi and J. Hafner, J. Phys. C **19**, 5799 (1986).
[13]W. Curtin and W. Ashcroft, Phys. Rev. A **32**, 2909 (1985).
[14]P. Tarazona, Phys. Rev. A **31**, 2672 (1985); **32**, 3148(E) (1985).
[15]A. D. J. Haymet, Annu. Rev. Phys. Chem. (in press); A. D. J. Haymet, Prog. Solid State Chem. **17**, 1 (1986).
[16]A. D. J. Haymet, Chem. Phys. Lett. **122**, 324 (1985).
[17]S. Sachdev and D. R. Nelson, Phys. Rev. B **32**, 1480 (1985).
[18]J. L. Barrat, M. Baus, and J. P. Hansen, Phys. Rev. Lett. **56**, 1063 (1986).
[19]S. J. Smithline and A. D. J. Haymet, J. Chem. Phys. (in press).
[20]A. D. J. Haymet and D. W. Oxtoby, J. Chem. Phys. **74**, 2559 (1981).
[21]D. W. Oxtoby and A. D. J. Haymet, J. Chem. Phys. **76**, 6262 (1982).
[22]B. B. Laird and A. D. J. Haymet, Mater. Res. Soc. Proc. **63**, 67 (1986).
[23]S. M. Moore and H. J. Raveche, J. Chem. Phys. **85**, 6039 (1986).
[24]W. H. Shih, Z. Q. Wang, X. C. Zeng, and D. Stroud, Phys. Rev. A **35**, 2611 (1987).
[25]Th. Klupsch, Ann. Phys. (Leipzig) **39**, 179 (1982); Th. Klupsch, Phys. Status Solidi B **109**, 535 (1982).
[26]W. A. Curtin, *A Theory of the Solid–Liquid Interface* (Standard Oil Co., 1987)
[27]P. Harrowell and D. W. Oxtoby, J. Chem. Phys. **86**, 2932 (1987).
[28]B. Bagchi, J. Chem. Phys. **82**, 5677 (1985).
[29]Y. Singh, J. P. Stoessel, and P. G. Wolynes, Phys. Rev. Lett. **54**, 1059 (1985).
[30]R. W. Hall and P. G. Wolynes, J. Chem. Phys. **86**, 2943 (1987).
[31]P. Harrowell and D. W. Oxtoby, J. Chem. Phys. **80**, 1639 (1984).
[32]M. Grant and J. D. Gunton, Phys. Rev. B **32**, 7299 (1985).
[33]M. V. Jaric, *Proceeding of the Xth International Workshop on Condensed Matter Theories*, edited by P. Vashishta (Plenum, New York, 1986); M. V. Jaric and U. Mohanty, Phys. Rev. Lett. **58**, 230 (1987).
[34]J. G. Kirkwood and E. Monroe, J. Chem. Phys. **8**, 845 (1940); **9**, 514 (1941); J. G. Kirkwood, in *Phase Transformations in Solids*, edited by R. Smoluchowski, J. E. Mayer, and W. A. Weyl (Wiley, New York 1951), p. 67.
[35]A. D. J. Haymet and D. W. Oxtoby, J. Chem. Phys. **84**, 1769 (1986).
[36]P. R. Harrowell, D. W. Oxtoby, and A. D. J. Haymet, J. Chem. Phys. **83**, 6058 (1985).
[37]J. K. Percus and G. J. Yevick, Phys. Rev. **110**, 1 (1958).
[38]E. Thiel, J. Chem. Phys. **39**, 474 (1963); M. S. Wertheim, Phys. Rev. Lett. **10**, 321 (1963).
[39]B. J. Alder and T. E. Wainwright, J. Chem. Phys. **31**, 459 (1959).
[40]W. Sutherland, Philos. Mag. **30**, 318 (1890).
[41]F. A. Lindemann, Phys. Z **11**, 609 (1910).
[42]J. E. Lennard-Jones, Physica **4**, 941 (1937).
[43]S. Goldman, J. Phys. Chem. **83**, 3033 (1979).
[44]J. J. Nicolas, K. E. Gubbins, W. B. Streett, and D. J. Tildesley, Mol. Phys. **37**, 1429 (1979).
[45]W. G. Madden and S. A. Rice, J. Chem. Phys. **72**, 4208 (1980).
[46]J. P. Hansen and L. Verlet, Phys. Rev. **184**, 151 (1969).
[47]R. K. Crawford and W. B. Daniels, Phys. Rev. Lett. **21**, 367 (1968).
[48]S. M. Shistov, Usp. Fiz. Nauk. **114**, 1 (1974).